# Polarized and Depolarized Light Scattering of Concentrated Polystyrene Solutions

**Wyn Brown***

*Department of Physical Chemistry, University of Uppsala, Box 532,*
*751 21 Uppsala, Sweden*

**Taco Nicolai**

*Laboratoire de Physico-Chimie Macromoleculaire, URA CNRS, Universite du Maine,*
*72017 Le Mans Cedex, France*

*Received September 20, 1993; Revised Manuscript Received February 18, 1994*®

ABSTRACT: Polarized and depolarized dynamic light scattering have been used to examine the dynamics of concentrated ($0.7 < C < 1.0$ g/mL) polystyrene solutions in dioctyl phthalate and toluene. Time–temperature superposition of the depolarized intensity correlation functions gave master curves covering more than 10 decades on the time scale. The polarized correlation functions are resolved by different procedures into relaxational and diffusive components having different temperature dependences. When the relaxation rate of the concentration fluctuations approaches the reorientational relaxation rate, the concentration fluctuations become $q$-independent; i.e., they become rate-determined by the polymer backbone mobility. With a small-molecule solvent such as toluene, however, a part of the concentration fluctuations relaxes faster than the orientational relaxation; i.e., the diffusion occurs in the free volume within the "frozen" network.

## Introduction

There has been considerable recent activity directed to an improved understanding of the dynamics of polymer–diluent systems and in particular to the properties of polymer-rich compositions close to the glass transition temperature ($T_g$) (see, for example, refs 1–9). Dynamic light scattering (DLS), dielectric relaxation (DR), depolarized Rayleigh scattering (DRS), Brillouin scattering (BS), ultrasound, and various dynamic mechanical techniques have been employed in concert. Recent reviews of the application of DLS to concentrated systems are provided by Chapters 9 and 10 of ref 9.

In bulk systems it is well established that the primary $\alpha$-relaxation dominates the correlation function which displays a very broad nonexponential decay. The latter is a localized main-chain motion and is therefore insensitive to the molecular weight. In the presence of a solvent, however, the dynamics become more complex and also reflect contributions from the concentration fluctuations, in addition to the longitudinal density and the local anisotropy fluctuations determined by segmental motions. Thus, on the one hand, concentration, density, and optical anisotropy fluctuations are present in the polarized ($V_V$) correlation function, while, on the other hand, anisotropy fluctuations due to segmental reorientational relaxation are observed in the depolarized ($V_H$) dynamic light scattering experiment. The density and orientational relaxation rates are $q$-independent since they do not reflect translational diffusion processes. Concentration fluctuations relax by cooperative diffusion, i.e., by local swelling and deswelling of the highly entangled transient network. For the samples studied here the terminal relaxation which is considered to occur by reptation of the chains is much slower than the time range covered by DLS. If the relaxation rate of the concentration fluctuations is appreciably slower than that of the orientational and density fluctuations, it is $q^2$-dependent. The present study shows that the relaxation rate of the concentration fluctuations becomes $q$-independent and controlled by the rate of the orientational fluctuations when their respective rates approach each other. Except at the highest polymer concentrations, the intensity of the depolarized scattered light is always much less than that of the polarized scattered light unless the solvent and polymer are index matched.

For bulk polymers the $\alpha$-relaxation, i.e., the chain backbone relaxation, is typified by a non-Arrhenius temperature dependence and this is conveniently analyzed in terms of the Vogel–Fulcher–Hesse–Tamman (VFHT) equation which is valid above the glass transition temperature (see, e.g., ref 12):

$$\log \langle \tau \rangle = \log \tau_0 + B/(T - T_0) \qquad (1)$$

where $\log \tau_0$, $B$, and $T_0$ are characteristic parameters describing the $T$-dependence of the average relaxation time $\langle \tau \rangle$ in terms of an activation energy (B) and the temperature $T_0$ which is the "ideal" glass transition temperature. The temperature dependence of the relaxation rate associated with the diffusional concentration fluctuations is considerably weaker at temperatures where it is slower than the $\alpha$-relaxation (see below). The characteristically different temperature dependences were clearly shown by Fytas et al. in the poly(cyclohexyl methacrylate)/dioctyl phthalate (DOP) system.[1,2]

Polarized DLS studies have recently been performed on two polymer solvent systems over a wide range of concentrations.[3,5] The relevant experimental results of these earlier studies are in qualitative agreement with the results presented here. However, some of the conclusions drawn need to be revised in light of the present study.

An investigation into the mobility of the solvent in the PS/toluene[13] and PS/DOP[10,11] systems using DRS and DR demonstrated the existence of two primary ($\alpha$-)relaxations reflecting the polymer and solvent dynamics, each having a broad distribution of relaxation times. The concentration and temperature dependence of the screening length was determined[6] using SANS and SAXS in the PS/toluene system, and these measurements showed that changes are marked in the vicinity of the concentration for which the glass temperature is close to the measurement temperature.

The present paper is devoted to a comparison between polarized ($V_V$) and depolarized ($V_H$) dynamic light scat-

® Abstract published in *Advance ACS Abstracts*, April 1, 1994.

0024-9297/94/2227-2470$04.50/0

tering measurements on polystyrene (PS) in dioctyl phthalate (DOP) and also in toluene over the accessible temperature range at polystyrene-rich concentrations. The former system is particularly convenient for studying polymer/solvent dynamics since, in addition to the techniques mentioned above, it is suited to rheological investigations, and these will be reported in a subsequent paper. In addition, the higher viscosity of DOP results in slower cooperative diffusion which simplifies DLS measurements in the high concentration regime.

## Experimental Section

Concentrated polystyrene solutions in chromatographic-grade (Merck) dioctyl phthalate and in toluene were prepared from carefully dried and vacuum-distilled styrene as previously described[3] by thermal polymerization of the monomer/solvent mixtures at 120 °C for 36 h directly in the measuring cells which were then sealed under vacuum. The conversion in the thermal polymerization was >97%. The weight-average molar mass is about $2.5 \times 10^5$ g/mol.

Dynamic light scattering measurements were made using the apparatus and technique described earlier[14] equipped with an Ar ion laser (Coherent Radiation Model Innova 300) emitting vertically polarized light with wavelength 488 nm and an ALV-5000 multibit, multi-$\tau$ full-digital autocorrelator.

For depolarized DLS the scattered light passed through a Glan-Thompson polarizer with an extinction coefficient of $10^{-7}$, whose orientation was adjusted to give a minimum scattering intensity for a dilute solution of high-MW polystyrene in ethyl acetate.

## Results

**Time–Temperature Superposition.** The measured depolarized intensity–intensity correlation functions relax over a broad time range independent of the scattering vector, $q$. With the ALV correlator a time range of about 8 decades (between $10^{-6}$ and 100 s) can be covered with good statistics, the upper limit being determined by the total duration of the measurement (usually ≤20 h). Since the characteristic relaxation time increases strongly with decreasing temperature, the main part of the correlogram is only visible in the time window of the correlator over a narrow temperature range. Direct analysis of correlation functions which cover only part of the relaxational process may consequently lead to systematic errors.

To circumvent this problem, we time-shift the depolarized correlograms: each correlogram at a particular temperature is shifted on the time axis so that it coincides with a central well-defined arbitrarily chosen correlogram. In this way a master correlogram is obtained covering an even wider time range. The master curve is then analyzed, for example by inverse Laplace transformation (ILT), yielding a characteristic relaxation time; the relaxation times at other temperatures are subsequently calculated from the shift factors. This procedure is inspired by the temperature–frequency shifts used in rheology and assumes that the shape of the correlograms is essentially the same in the temperature range investigated. In fact the validity of this assumption is verified by the good agreement between the correlograms in the time ranges in which they overlap.

The above approach is illustrated by data for the 0.9 g/mL PS/toluene system. The observed depolarized correlograms at a number of temperatures are shown in Figure 1a. The master curve has been obtained in this case by shifting each correlogram relative to that at 60 °C. A fit procedure has been used to obtain the best agreement in the overlap region. Three fit parameters are required to obtain good agreement: the time shift parameter, $K$, the base line, $B$, and the relative amplitude, $A$. $B$ is necessary to correct for varying amounts of residual relaxation outside the time window of the correlator which is small if the sample is kept for a longer equilibration time at each temperature. The floating amplitude allows for comparison between measurements made at different apparatus settings but varies little between experiments at the same settings.

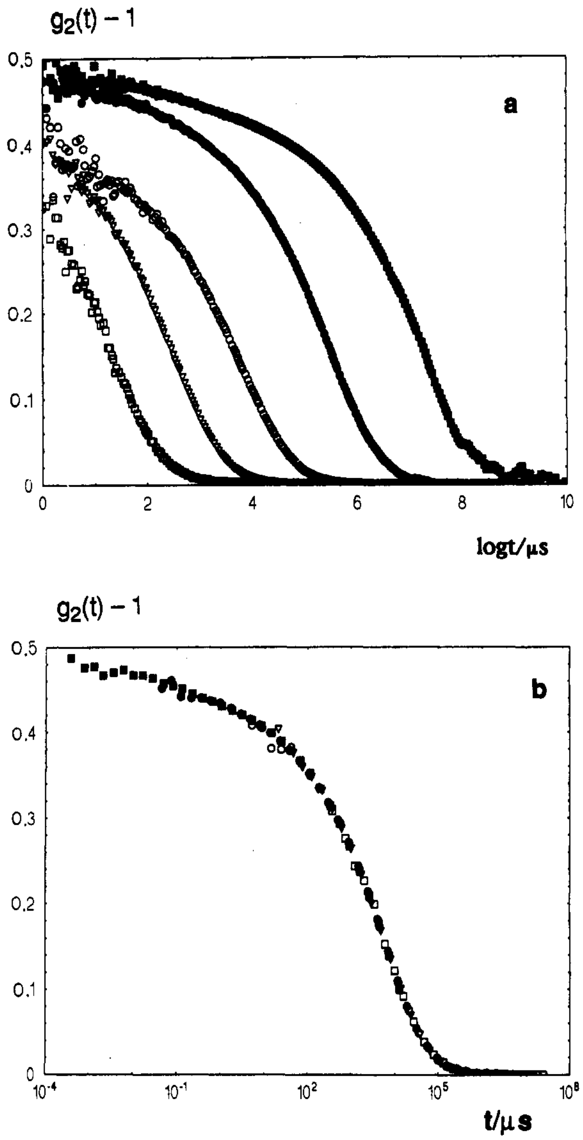

**Figure 1.** (a) Depolarized intensity autocorrelation functions for polystyrene in toluene; $C = 0.9$ g/mL, $\theta = 90°$. Temperatures from left to right: 70, 60, 50, 40, 30 °C. (b) Same data time-shifted relative to the correlation function at 60 °C.

**Table 1. Fit Parameters Used in the Time–Temperature Shifts of Correlation Functions Measured on 0.9 g/mL Polystyrene in Toluene with Respect to the Measurement at 60 °C (See Text)**

| $T$ (°C) | log($K$) | $A$ | $B$ |
|---|---|---|---|
| 30 | −4.82 | 0.99 | 0 |
| 40 | −2.03 | 0.96 | 0 |
| 50 | −1.32 | 1.1 | 0 |
| 60 | 0 | 1 | $1.9 \times 10^{-3}$ |
| 70 | 1.17 | 0.99 | $2.8 \times 10^{-3}$ |

The resulting master curve, covering more than 10 decades on the time scale, is shown in Figure 1b. The parameters obtained in the fitting are summarized in Table 1. $K$ is only weakly-dependent on $B$ and $A$ and is essentially unchanged if $B$ is set to zero and $A$ to unity. The intercept of the master curve is smaller by less than 20% compared to the value given by the apparatus settings. This reduction is partly due to inhomogeneities frozen on the time scale of the measurement and partly due to relaxations

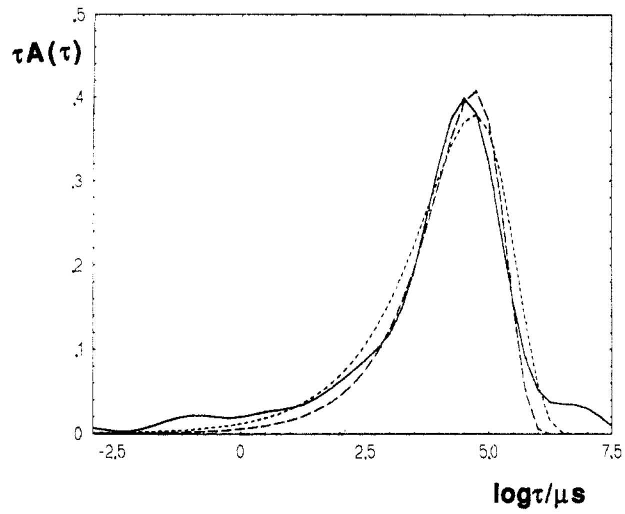

**Figure 2.** Relaxation time distributions corresponding to the master correlation function shown in Figure 1b obtained from an ILT (solid), KWW with $\beta$ = 0.45 (long dashes), and KWW with $\beta$ = 0.385 (short dashes).

faster than 1 µs. The time-averaged intensity is independent of the position of the scattering volume if the intensity is averaged over times much longer than the slowest relaxational process. The necessary averaging time becomes very large close to $T_g$, and below $T_g$ the samples are necessarily nonergodic due to frozen-in density and concentration fluctuations. However, above $T_g$ all the samples are ergodic and there is no heterodyning contribution.

Master curves were analyzed by taking the inverse Laplace transform (ILT) and employing the routine REPES,[15] to obtain the corresponding relaxation time distributions. This program is similar to Provencher's CONTIN[16] except that the former directly minimizes the sum of the squared differences between experimental and calculated intensity–intensity $g_2(t)$ correlation functions using nonlinear programming. For a system exhibiting a distribution of relaxation times, the field autocorrelation function $g_1(t)$ ($g_2(t) = g_1^2(t) + 1$) is described by a continuous function of the relaxation time $\tau$ using the Laplace transform:

$$g_1(t) = \int_0^\infty A(\tau) \exp(-t/\tau)\, d\tau \qquad (2)$$

Relaxation time distributions are given, in the form of $\tau A(\tau)$ versus log $\tau$ plots, with $\tau A(\tau)$ in arbitrary units. This provides an equal area representation. The fitting procedure yields excellent fits but represents broad distributions by multiple peaks when no smoothing is applied. Even if a large amount of smoothing is applied, a residual "waviness" may still be visible. This is caused by a small amount of nonrandom noise produced by the correlator if the correlation function is characterized by a very broad relaxation time distribution.[17] The effect of the nonrandom noise is difficult to calculate and cannot as yet be taken into account in the fitting procedure.

To facilitate comparison with DLS results reported in the literature, we have also analyzed the data by fits to a so-called Kohlrausch–Williams–Watts (KWW) function:

$$g_2(t) = (A \exp[-(t/\tau)^\beta] + B)^2 \qquad (3)$$

This function gives, however, only an approximate description of the measured correlograms. Deviations are apparent on both the fast and the slow sides. This is illustrated in Figure 2, where the relaxation time spectra corresponding to simulated KWW functions are compared with the ILT result for the 0.9 g/mL PS/toluene system. The stretched exponential with $\beta$ = 0.45 best describes the central part of the distribution, while $\beta$ = 0.385 results from a fit to all of the data. Deviations from a single stretched exponential are more important in the PS/DOP system and increase with increasing solvent concentration (see below).

For very broad relaxation time distributions the choice of a characteristic relaxation time is somewhat arbitrary. We have chosen here to take the maximum of the relaxation time distribution. In contrast to the average relaxation time, this value is insensitive to the exclusion of points at the fast or slow ends of the correlogram. This value was found to be very close to the result from a forced fit to eq 3 in all cases.

**Polystyrene in DOP. Depolarized Light Scattering.** Depolarized scattered light intensity autocorrelation functions have been measured for bulk polystyrene and for three concentrations of PS in DOP: 0.9, 0.8, and 0.7 g/mL.

Master correlograms obtained from a time–temperature superposition are shown in Figure 3a–d. With increasing solvent concentration, the correlogram deviates increasingly from a single KWW function. Forced fitting to a single KWW function then yields decreasing values for the stretched exponential, $\beta$, with increasing solvent concentration. However, excluding data from the fast end of the correlograms improves the fit and increases the value of $\beta$. Therefore, $\beta$ is not the most appropriate parameter to characterize the relaxation time distributions. The corresponding relaxation spectra obtained from an ILT (see Figure 3e,f) show clearly that, while the slow end of the relaxation spectra remain essentially unchanged, additional fast modes appear with increasing amplitude when the solvent content is increased.

Floudas et al.[10] recently reported results of depolarized light scattering measurements on a sample containing 0.5 g/mL of PS in DOP. As anticipated, an even larger contribution of fast relaxation times is observed for this system. Using dielectric relaxation, they show that the orientational relaxation spectrum of DOP is slowed down and broadened by the presence of PS. Thus part of the reorientational relaxation spectrum of DOP becomes visible in the time window of the correlator. Small systematic deviations at the fast end of the correlograms when applying time–temperature superposition indicate that the temperature dependences of the two modes are not identical.

Characteristic reorientational relaxation times, $\tau_{or}$, obtained from the maxima in the depolarized relaxation time spectra, are plotted as a function of temperature in Figure 4a. As mentioned above, the peak positions are insensitive to the deletion of data points at the fast end of the correlograms. Since the maximum position is uninfluenced by the presence of additional fast modes, it remains characteristic of the main-chain orientational relaxations of polystyrene. Lindsey et al.[19] report average relaxation times for bulk polystyrene as a function of temperature. These data, after correction for the difference between the average relaxation time and the peak position in the distribution, are included in Figure 4a for comparison.

The characteristic relaxation times decrease strongly with increasing solvent content, but the temperature dependence remains the same within experimental error. This is shown in Figure 4b where a temperature shift has been performed to bring the data at different concentra-

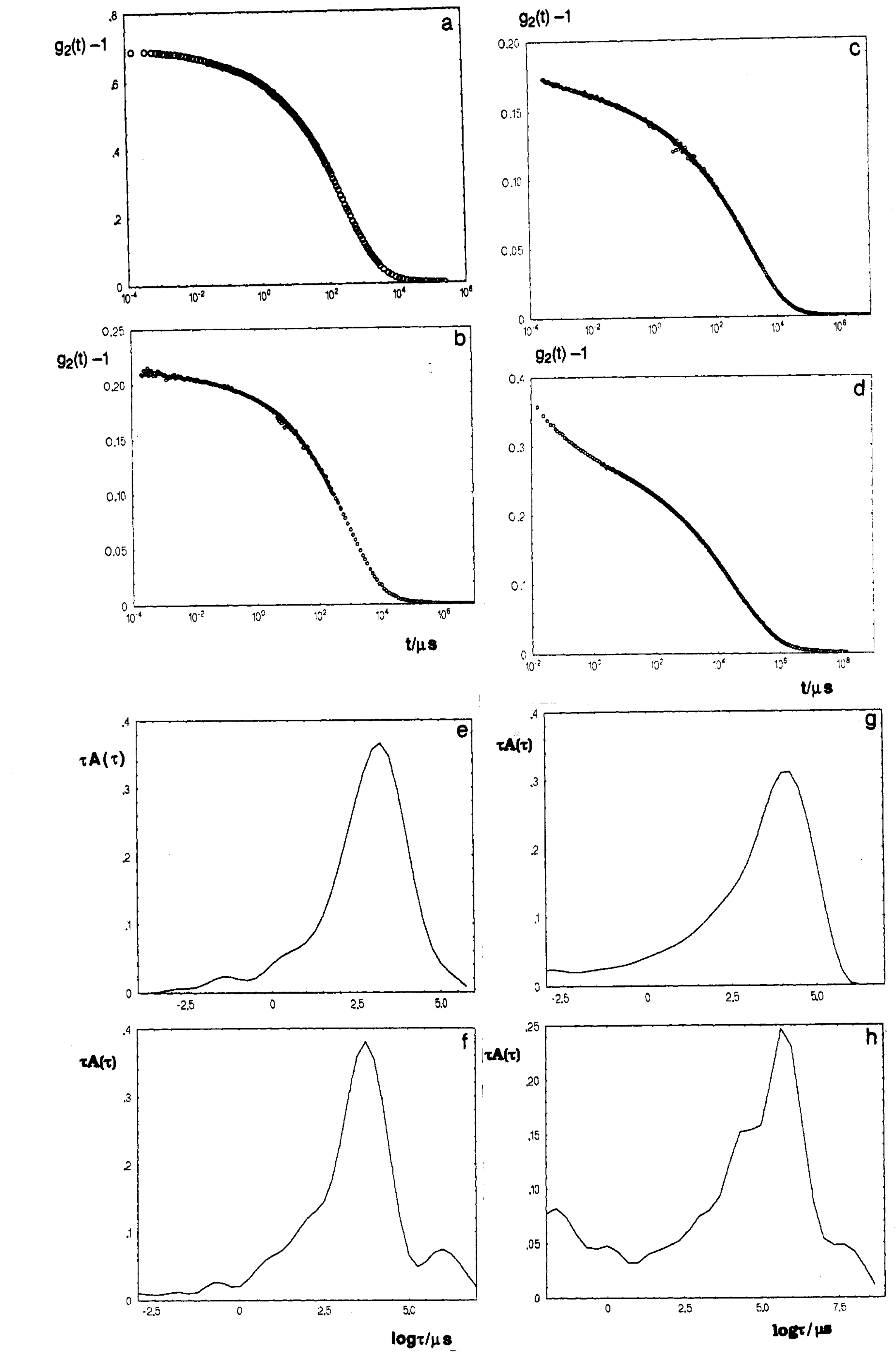

**Figure 3.** (a–d) Depolarized master correlation functions for polystyrene in DOP. Each master curve at a given concentration is made up of five time-shifted correlograms at different temperatures at $\theta = 90°$. Parts a–d represent bulk PS, 0.9, 0.8, and 0.7 g/mL, respectively. (e–h) Relaxation time distributions corresponding to the master correlation functions shown in parts a–d obtained from ILT. Parts e–h represent bulk PS, 0.9, 0.8, and 0.7 g/mL, respectively.

tions into coincidence with the bulk polystyrene data. The shift factors necessary for the superposition are 34, 65, and 85 °C for 0.9, 0.8, and 0.7 g/mL of polystyrene in DOP, respectively. An interpretation of these data

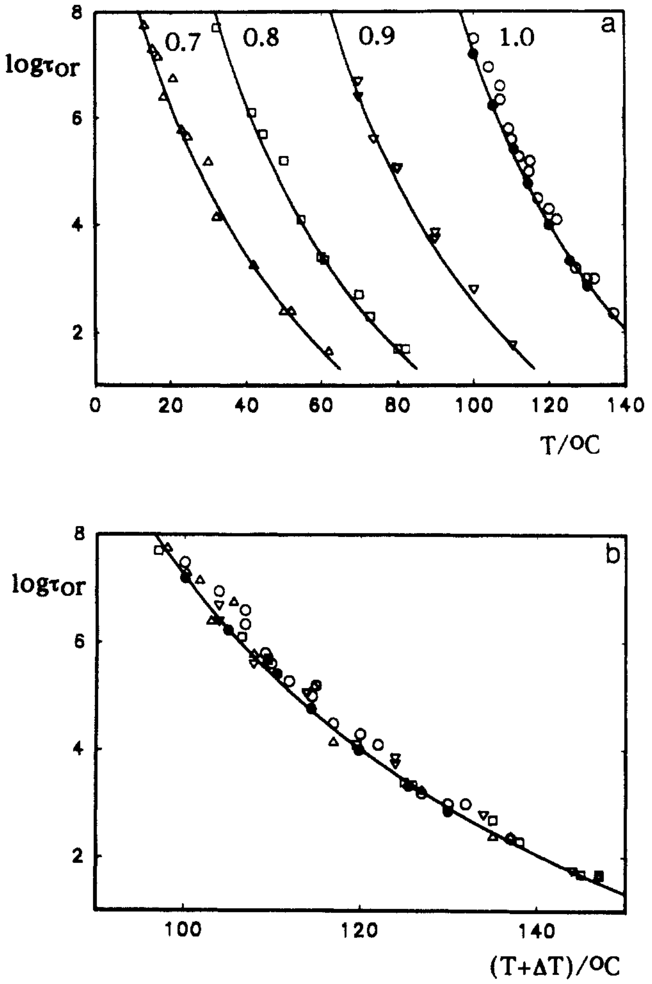

**Figure 4.** (a) Characteristic relaxation times from depolarized (V$_\mathrm{H}$) measurements plotted as a function of temperature for bulk polystyrene and the three concentrations in DOP shown. Filled points from ref 19. (The solid lines are guides to the eye.) (b) Same data temperature-shifted with respect to bulk polystyrene to give a master curve.

together with the results of the PS/toluene system is given below.

**Polystyrene in DOP. Polarized Light Scattering.** Vertically, $I_{\mathrm{v_v}}$, or nonpolarized, $I_{\mathrm{v}-}$, scattered light contains an isotropic component, $I_{\mathrm{iso}}$, in addition to the anisotropic component, $I_{\mathrm{v_h}}$, observed in depolarized light scattering. For bulk polystyrene we find $I_{\mathrm{v_h}}/I_{\mathrm{v_v}}$ to be about 0.5, which implies that the contribution of the isotropic scattering to $I_{\mathrm{v_v}}$ or $I_{\mathrm{v}-}$ is rather small. Lindsey et al.[19] also reported a ratio of about 0.5, while Koch at al.[5] found much lower values. The latter result is probably due to different sample preparation which could give large-scale inhomogeneities in the samples.

Isotropic scattering in bulk polystyrene, as long as it is not caused by inhomogeneities or impurities, is due to density fluctuations. The relaxation spectrum associated with these fluctuations is very similar to that associated with orientational fluctuations due to the strong coupling between the two dynamical processes.

When solvent is added, concentration fluctuations cause $I_{\mathrm{iso}}$ to increase while $I_{\mathrm{v_h}}$ varies only weakly depending on the relative values of $I_{\mathrm{v_h}}$ for the polymer and the solvent. The scattering due to concentration fluctuations is related to the inverse osmotic compressibility $(\delta\pi/\delta c)$:[18] $I = Kc(\delta\pi/\delta c)^{-1}$, where $K$ is a contrast factor which depends on the experimental conditions and the refractive index difference between the solvent and the polymer. The increase of $I_{\mathrm{iso}}$ is very strong in the case of PS in DOP as is shown in Figure 5 where $I_{\mathrm{v}-}$ is plotted relative to the value for bulk PS. For the good solvent system PS/toluene the increase is not as strong due to the better solvent quality. The polarized and depolarized scattering intensities of bulk polystyrene, DOP, and toluene are all very similar so that it is not necessary to take into account the variation in the scattering of the pure components at different compositions. Both polarized and depolarized scattered light intensities are independent of the temperature within experimental error over the temperature range covered in this study.

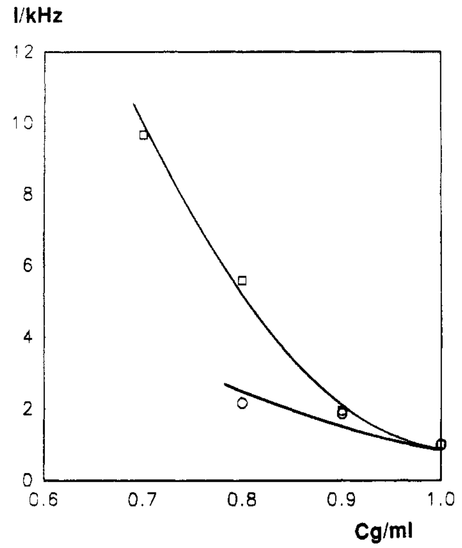

**Figure 5.** Total scattered light intensities using vertically polarized incident light and no analyzer plotted as a function of the PS concentration in DOP (squares) and toluene (circles). The data are normalized by the value for bulk PS.

Since the Raman and Brillouin scattering contributions are of much higher frequency, the correlation function of polarized scattered light may be written as the sum of three components due to (1) orientational fluctuations, (2) density fluctuations, and (3) concentration fluctuations. The correlation functions measured on bulk polystyrene in the V$_\mathrm{V}$ and V$_\mathrm{H}$ modes at the same temperature are closely similar except for the more important contribution of very slow structural relaxations in the V$_\mathrm{V}$ mode. In an earlier DLS study on bulk polystyrene, Lindsey et al.[19] reported a slightly broader relaxation time distribution in the V$_\mathrm{V}$ compared to the V$_\mathrm{H}$ mode. That this difference is very small is clear from the comparison of V$_\mathrm{V}$ and V$_\mathrm{H}$ master correlograms shown in Figure 6 (each curve is a composite of data at a series of five temperatures shifted relative to the data at 127 °C). Due to the different definition of the characteristic relaxation time, the values of $\tau$ reported by these authors are systematically somewhat higher than the values given here but the temperature dependence is the same. The contribution of concentration fluctuations increases with increasing solvent concentration and the relative amplitude happens to be about 0.5 for 0.9 g/mL of PS in DOP. This system is therefore suitable for demonstrating the various contributions to the correlation function.

Correlograms obtained for this system at scattering angle 90° are shown in Figure 7a for various temperatures. Two relaxational processes can be clearly distinguished at the higher temperatures. The faster, relatively broad component ($\tau_{\mathrm{or}}$) is due to a combination of both the orientational and the density fluctuations, the relative contribution of the latter being rather small. This is shown in Figure 7b where correlograms obtained with polarized and depolarized scattered light are compared at the same

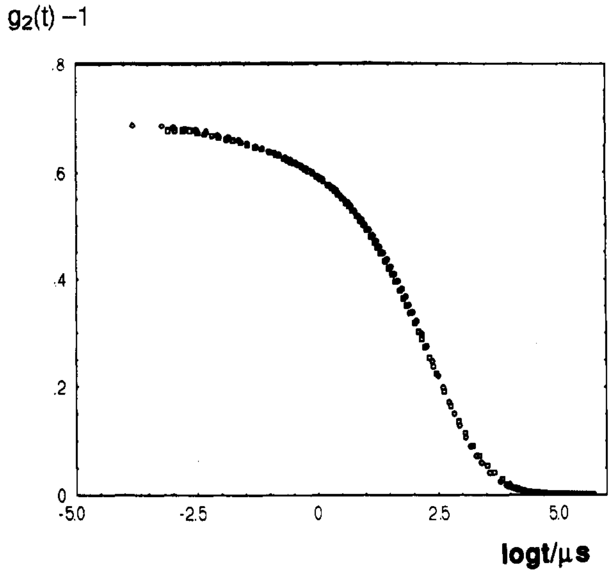

**Figure 6.** Depolarized master correlogram and polarized master correlogram for bulk polystyrene measured at $\theta = 90°$. Each correlogram is a composite of data at the five temperatures 104, 107, 112, 127, and 137 °C which have been time-shifted relative to the correlation function at 127 °C. There are insignificant differences between the data in the $V_V$ (□) and $V_H$ (○) geometries.

temperature. The slower mode in the $V_V$ is much narrower and is due to concentration fluctuations ($\tau_{con}$). The two modes have different temperature dependences so that time–temperature shifts can only be applied to part of the correlograms. Shift factors needed to obtain superposition of the fast end of the correlograms are very close to the corresponding values for depolarized light scattering.

Three analysis methods have been applied:

(a) ILT using REPES. The relaxation time distributions show a narrow peak together with a broad rather ill-defined distribution. When the temperature is increased, the two distributions merge. A characteristic relaxation time is again defined as the maximum in the relaxation time spectrum.

(b) A fit to a double KWW function, in order to facilitate comparison with DLS results on similar systems reported in the literature.

(c) A fit to a combination of a generalized exponential (GEX) plus a Gaussian distribution in log time (Gauss-GEX). The Gauss represents the narrow distribution, while the generalized exponential has an additional degree of freedom compared to the KWW equation to represent the broad distribution. However, a physical meaning is not attached to the parameters of this fit. Details of the application of this function can be found in ref 3. We have used this method to obtain smoothed graphical representations of the relaxation time distributions.

Methods b and c assume that the correlation function can be described by a bimodal relaxation time distribution and neglect the influence of additional fast modes detected in the depolarized light scattering: see above. Nevertheless, both methods give good descriptions of the experimental data (see, e.g., Figures 14a and 15a), although with lower statistical accuracy than method a. Relaxation time distributions resulting from method c are given in parts a–d of Figure 8 which clearly show the different temperature dependences of the two modes.

Table 2 summarizes the characteristic relaxation times for the broad ($\tau_{or}$) and narrow ($\tau_{con}$) components from the polarized correlograms shown in Figure 7a using each method, together with the results from depolarized light scattering measurements on the same system. It is clear that the characteristic time for the narrow relaxation mode is almost independent of the analysis method used, while the variations observed for the broad relaxation are probably due to the poorer definition of this mode in the polarized measurements compared to the depolarized measurements.

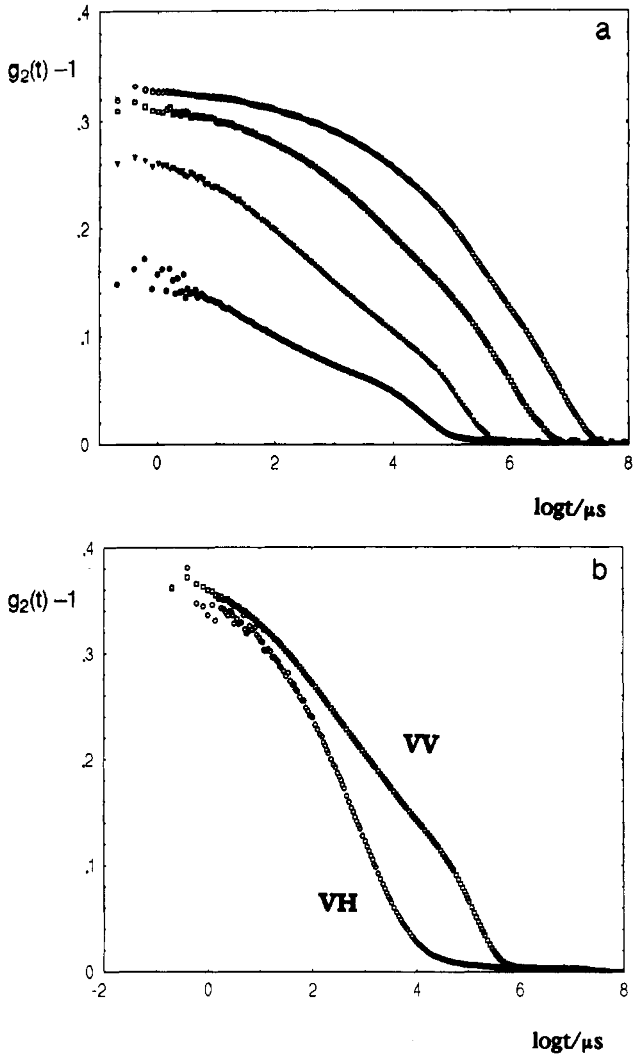

**Figure 7.** (a) Polarized intensity autocorrelation functions for polystyrene in DOP; $C = 0.9$ g/mL, $\theta = 90°$. Temperatures from left to right: 100, 90, 80, 70 °C. (b) Comparison of depolarized (left) and polarized (right) correlation functions on the same system: 0.9 g/mL PS/DOP at 90 °C and $\theta = 90°$.

The relative amplitude of the slower mode increases with increasing solvent concentration: 0.45 ± 0.5, 0.85 ± 0.5, and 0.9 ± 0.5 for 0.9, 0.8, and 0.7 g/mL of PS in DOP, respectively, independent of the temperature and scattering angle. The increase is compatible with the relative increase of the total scattered light intensity. The exponent $\beta$ obtained from fits to a double KWW function is about 0.3 for the fast mode, while for the slow mode $\beta$ decreases from a value close to unity, when the modes are well-separated, to about 0.6, when they overlap.

If the two modes are well-separated, the narrow mode is $q^2$-dependent, indicating a translational process, while the broad mode is $q$-independent, as shown in Figure 9 where the three correlation functions have been normalized to the same intercept. A detailed study of the $q$-dependence was made for the sample with $C = 0.7$ g/mL for which the contribution of concentration fluctuations is dominant; see Figure 10.

At 45 °C $\tau_{con}$ is $q^2$-dependent and longer than $\tau_{or}$ over the whole accessible $q$-range. At 35 °C $\tau_{con}$ is $q$-independent and close to $\tau_{or}$ at higher $q$-values while $q^2$-dependent

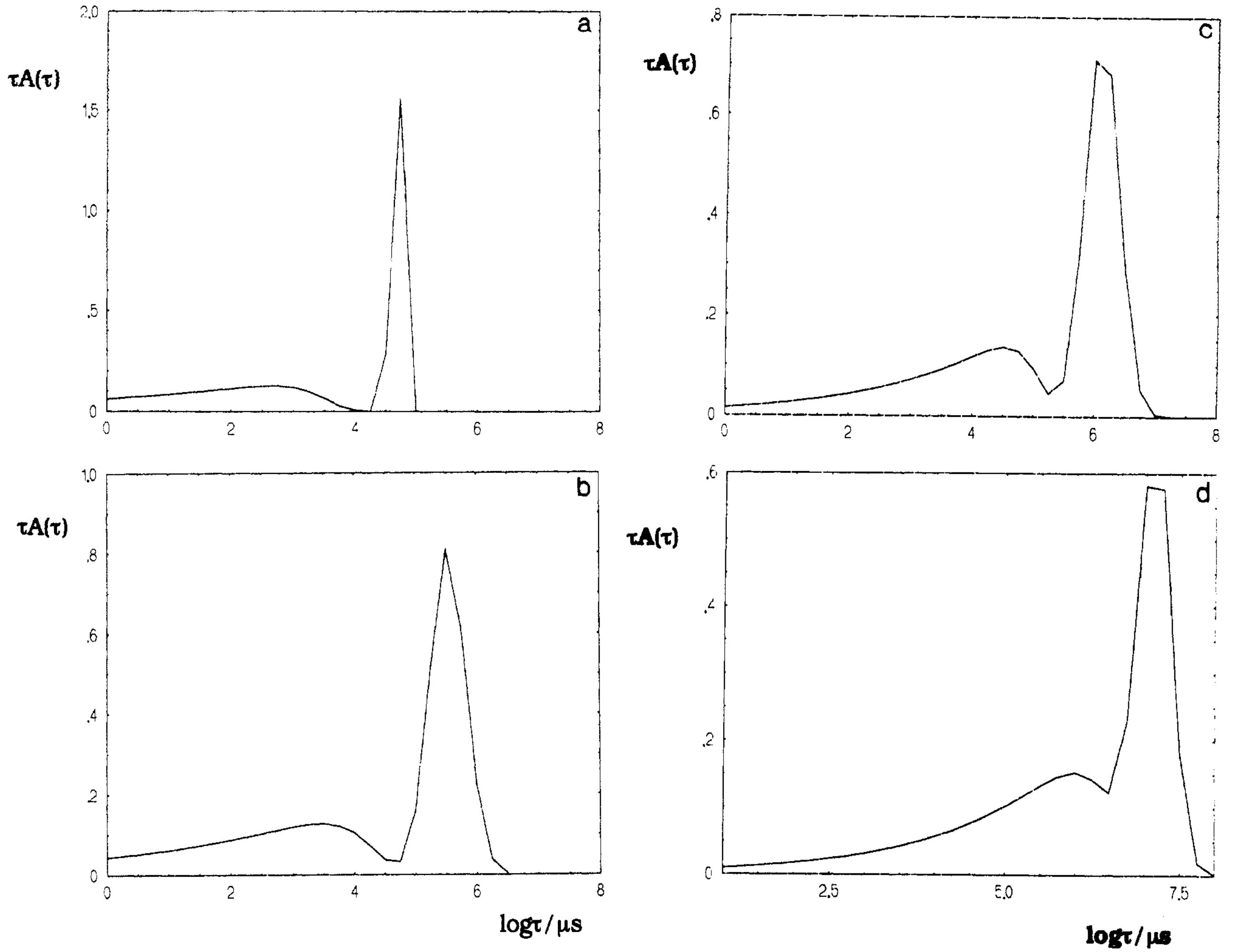

**Figure 8.** Relaxation time distributions corresponding to the correlation functions (polystyrene/DOP) shown in Figure 7a obtained from a Gauss-GEX analysis (see text). Parts a–d show the results at 100, 90, 80, and 70 °C, respectively.

**Table 2. Comparison of Characteristic Relaxation Times of the Narrow and Broad Modes in the Polarized Correlation Functions (PS/DOP; $C$ = 0.9 g/mL; $\theta$ = 90°) Obtained by Different Analysis Methods**

| $T$ (°C) | $\log(\tau)_n$[a] | $\log(\tau)_n$[b] | $\log(\tau)_n$[c] | $\log(\tau)_b$[a] | $\log(\tau)_b$[b] | $\log(\tau)_b$[c] | $\log(\tau)_b$[d] |
|---|---|---|---|---|---|---|---|
| 70 | 7.3 | 7.1 | 7.3 | 6.0 | 6.2 | 5.8 | 6.4 |
| 80 | 6.6 | 6.5 | 6.4 | 4.9 | 4.7 | 4.2 | 5.0 |
| 90 | 5.5 | 5.3 | 5.5 | 3.3 | 3.3 | 3.0 | 3.7 |
| 100 | 4.7 | 4.7 | 4.7 | 2.5 | 2.5 | 2.1 | 2.8 |

[a] From a time–temperature shift. [b] From a Gauss-GEX fit (see text). [c] From a double stretched exponential fit. [d] From depolarized light scattering.

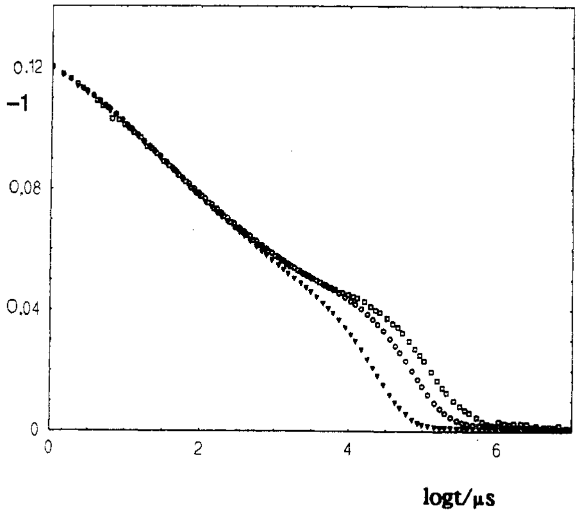

**Figure 9.** Polarized intensity autocorrelation functions for polystyrene in DOP; $C$ = 0.9 g/mL at 100 °C. Scattering angles from left to right: 100, 60, and 40°.

and longer than $\tau_{or}$ at lower $q$-values. At lower temperatures the $q$-independent range extends to lower $q$-values. It may thus be concluded that the relaxation of concentration fluctuations occurs by translational diffusion when the relaxation time of this process is longer than $\tau_{or}$. When $\tau_{con}$ closely approaches $\tau_{or}$, the relaxation rate of the concentration fluctuations is controlled by the relaxation rate of the orientational and density fluctuations.

As mentioned above, the relaxation time distribution characterizing the concentration fluctuations, $A(\tau_{con})$, is relatively narrow when $q^2$-dependent and somewhat broader when $q$-independent. A broadening may be expected if the relaxation rate of concentration fluctuations is determined by density and orientational fluctuations. However, $A(\tau_{con})$ remains much narrower than $A(\tau_{or})$ as shown in Figure 11 in which relaxation time distributions from polarized and depolarized DLS are compared for the 0.7 g/mL PS/DOP system. Apparently the $q$-independent rate of the concentration fluctuations is determined by the slower part of the orientational and density fluctuations, i.e., relaxation of the chain backbone.

Characteristic relaxation times ($\tau_{con}$) derived from data measured at scattering angle 90° in the $V_V$ geometry are plotted in Figure 12a as a function of temperature for three concentrations of PS in DOP together with the depolarized light scattering results ($\tau_{or}$). As we have seen, the latter are close to the characteristic times for the broad mode in polarized DLS but are obtained with better precision, especially when the relative amplitude of this

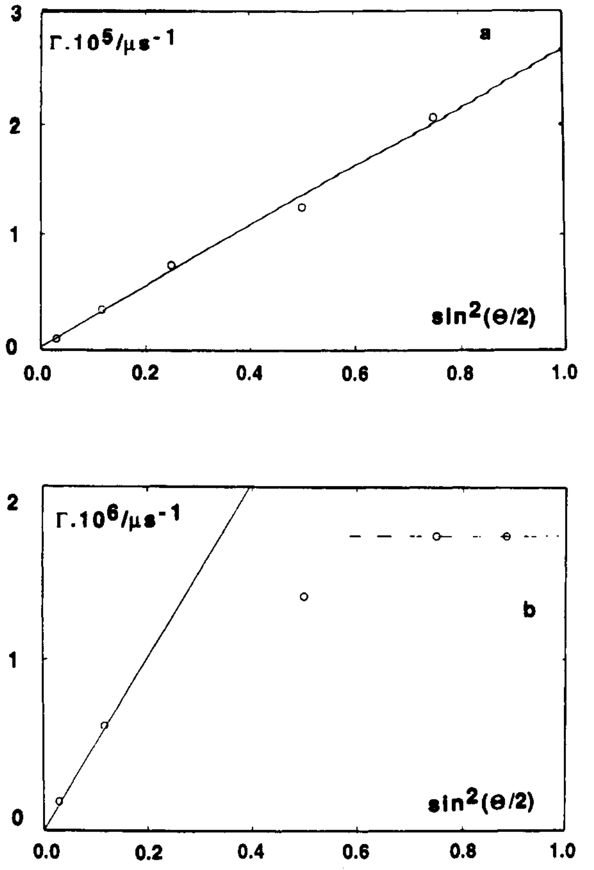

**Figure 10.** Plots of relaxation rate $\Gamma = 1/\tau$ versus $\sin^2(\theta/2)$ for PS/DOP at $C = 0.7$ g/mL in the polarized mode at (a) 45 °C and (b) 35 °C. The slope of the solid lines represents the diffusion coefficient.

mode becomes small. It is clear from Figure 12a that $\tau_{or}$ and $\tau_{con}$ have different temperature dependences and merge at low temperatures whereupon $\tau_{con}$ follows $\tau_{or}$. By applying the same temperature shift to both $\tau_{or}$ and $\tau_{con}$, an approximate master curve is obtained representing all three concentrations; see Figure 12b.

**Polystyrene in Toluene.** Many of the features observed for the PS/DOP system are also observed for the PS/toluene system. Depolarized DLS on two concentrations (0.9 and 0.8 g/mL) shows similar broad relaxation time distributions. The temperature dependence of $\tau_{or}$ is close to that observed in DOP. The concentration dependence, however, is much stronger as is expected since the glass transition temperature ($T_g$) decreases much more with the addition of toluene than with DOP.

The temperature shifts relative to bulk polystyrene are 65 and 94 °C for 0.9 and 0.8 g/mL, respectively, which correspond to the shifts in $T_g$ measured by DSC.[3]

An Arrhenius plot of the relaxation rates for both the toluene and DOP systems is given in Figure 13. All data are shifted to the bulk polystyrene values using the shift factors given above. A fit to the VHFT equation shown by the full line yields $\log\langle\tau\rangle = -13.1 + 972/(T - 307)$, with $\tau$ given in seconds. The relation given in ref 12 also describes the data well within experimental error.

At higher temperatures, polarized DLS again shows a broad relaxational mode followed by a narrow $q^2$-dependent mode; see Figure 14a,b. However, at the lower temperatures a narrow $q^2$-dependent mode precedes the broad mode; see Figure 15a,b. The relaxation time of the broad mode is, within experimental error, identical to the corresponding value of $\tau_{or}$ observed in depolarized DLS. In the case of the 0.9 g/mL PS/toluene system, the relative amplitude of the narrow mode ($\tau_{con}$) is about 0.3 when it follows the broad mode and about 0.05 when it precedes it, independent of temperature and scattering angle. It appears that a small part of the concentration fluctuations can relax faster than $\tau_{or}$. Relaxation times of the narrow mode ($\tau_{con}$) are compared to $\tau_{or}$ in Figure 16a. The measurements were performed at different scattering angles in order to obtain a better separation of the two modes and are reduced to 90° using the $q^2$ dependence of the narrow mode and the $q$ independence of the broad mode. In the case of 0.8 g/mL PS/toluene, a similar pattern is observed; see Figure 16b. The temperature dependence of the diffusional mode is difficult to measure accurately, because the relaxation times are very short at the temperatures at which the two modes are well separated.

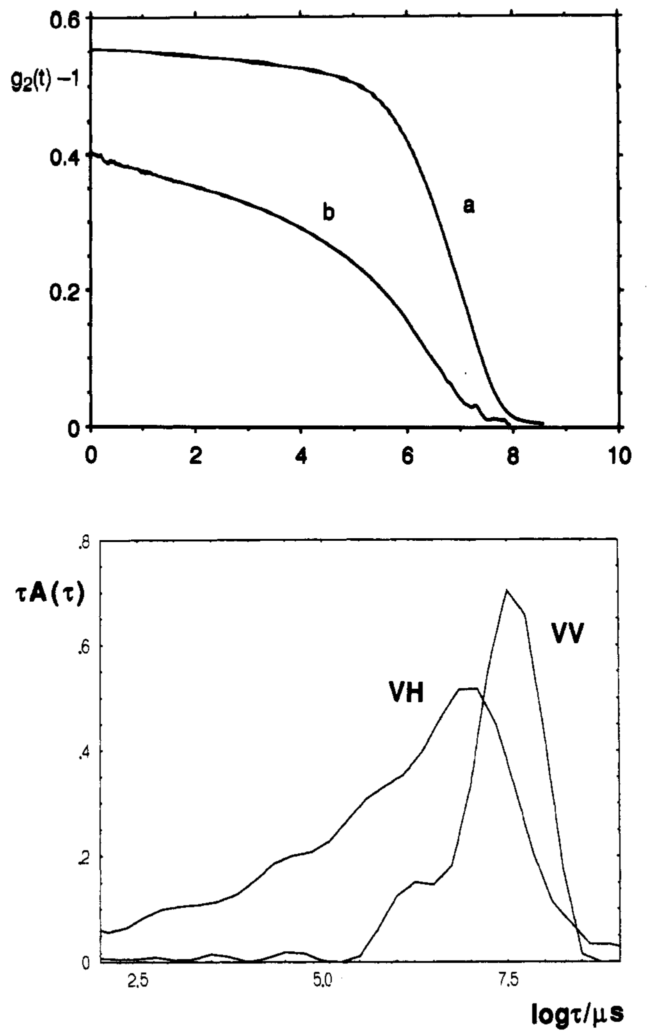

**Figure 11.** Comparison of (a) correlation functions and (b) relaxation time distributions obtained by ILT of polarized and depolarized correlation functions of 0.7 g/mL PS/DOP at 20 °C when both are $q$-independent over the accessible $q$-range.

## Discussion and Conclusion

The correlation functions for bulk polystyrene in the depolarized mode are closely described by a single stretched exponential in agreement with earlier literature (e.g., ref 12). Small deviations only become apparent if the correlation function is determined over a very large time range, and Patterson has given a discussion of this aspect. In the solutions, deviations from a single stretched exponential increase, however, with increasing solvent concentration and are apparent at both the slow and fast ends of the correlation functions. The deviation at the slow end is probably due to restructuring of the transient gel which occurs on a time scale slower than the density

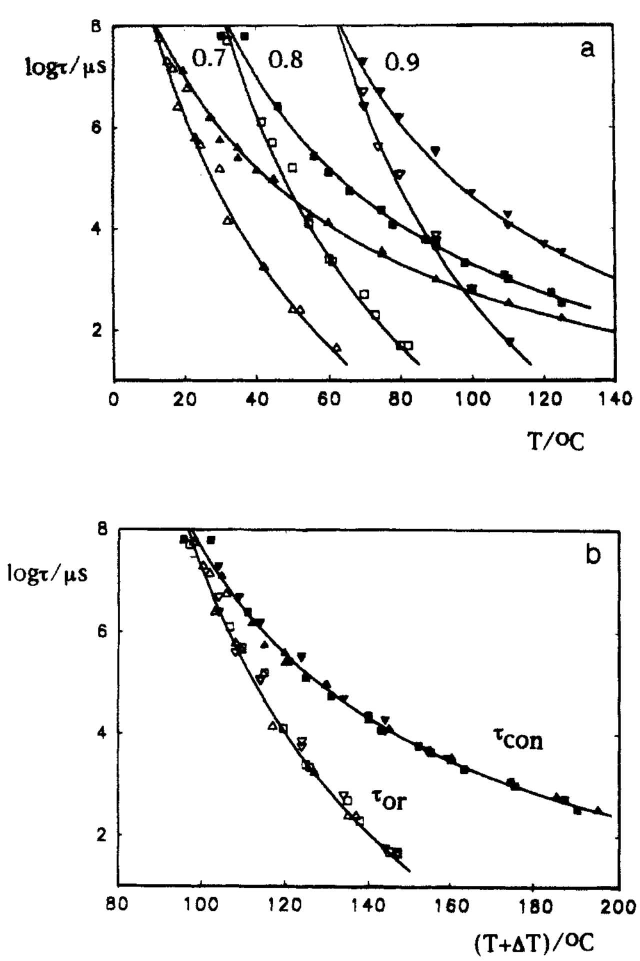

**Figure 12.** (a) Characteristic relaxation times from polarized ($\tau_{con}$) (filled points) and depolarized ($\tau_{or}$) (open points) data plotted as a function of temperature for the three concentrations in DOP shown θ = 90°. (The solid lines are guides to the eye.) (b) The data in Figure 12a temperature-shifted with respect to data for bulk polystyrene using the same shift factors for both modes to give master curves.

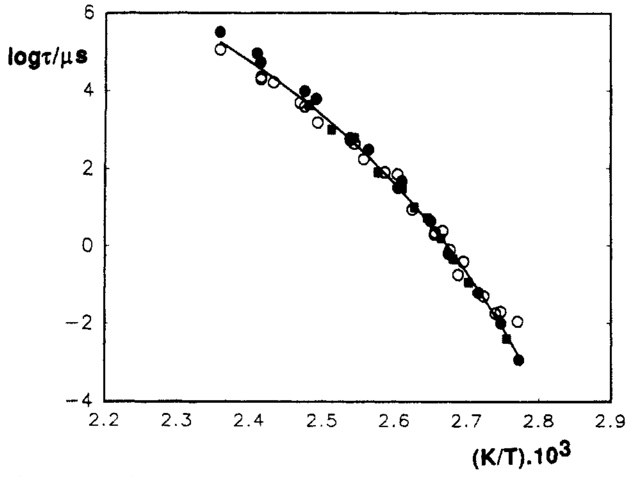

**Figure 13.** Arrhenius plot of the depolarized data for bulk PS (squares), the PS/Toluene (open circles), and PS/DOP (filled circles) systems at different concentrations. All data have been shifted on the temperature axis relative to data for bulk PS. The solid line represents a fit to VHFT (see eq 1), with $\tau_0 = -13.1$ s, $B = 972$ K, and $T = 307$ K.

fluctuations. However, above $T_g$ the samples are ergodic and the measurements are not influenced by heterodyning. The deviations at short times, which increase with increasing solvent concentration, have a different origin. The relaxation time distribution of polystyrene is modified by the presence of the solvent which yields a larger amplitude of relatively fast relaxations. For example, in the case of DOP, the relaxation of the solvent, which is itself modified by the presence of polystyrene, becomes visible in the time window of the correlator at low temperatures. Floudas et al.[10] have measured a 0.5 g/mL solution of polystyrene in DOP and shown that over a limited temperature range both relaxations are at least partly probed in the time window of the correlator. Since the two relaxation processes have different temperature dependences, a time–temperature superposition cannot be valid for the whole correlogram. The deviations are nevertheless small and, where they occur, the slower part of the correlogram which is dominated by the relaxation of polystyrene can be used in the superposition procedure.

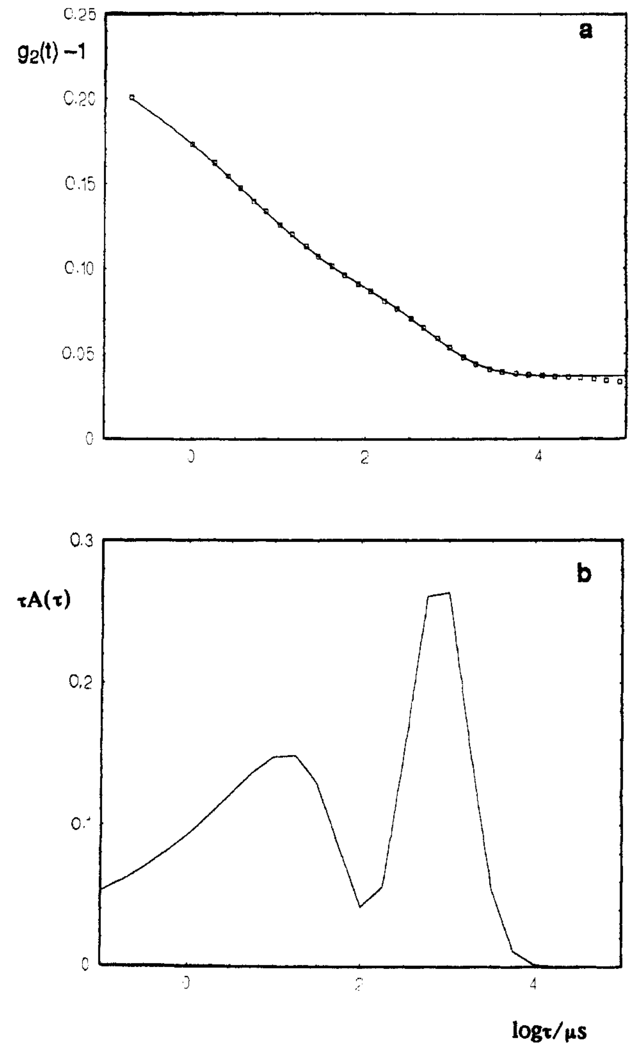

**Figure 14.** (a) Polarized intensity autocorrelation function for polystyrene in toluene; $C = 0.9$ g/mL at 100 °C and θ = 90°. The broad $q$-independent mode is followed by a slow diffusive mode. (b) Corresponding relaxation time distribution obtained from a Gauss-GEX analysis (see text).

In the polarized mode an additional relaxation time distribution due to concentration fluctuations is observed when the solvent is present. The characteristic relaxation time is then either much slower than that of the orientational and density fluctuations, in which case it is $q^2$-dependent, or close to the latter, in which case it is $q$-independent. In the case of toluene a small part of the concentration fluctuations relax faster than the orientational relaxations, i.e., in the frozen network. For DOP such a fast relaxation has not been observed. Diffusional processes both faster and slower than the orientational relaxations have been observed for other systems, but only for polystyrene in toluene are both observed for the same system.[3,22]

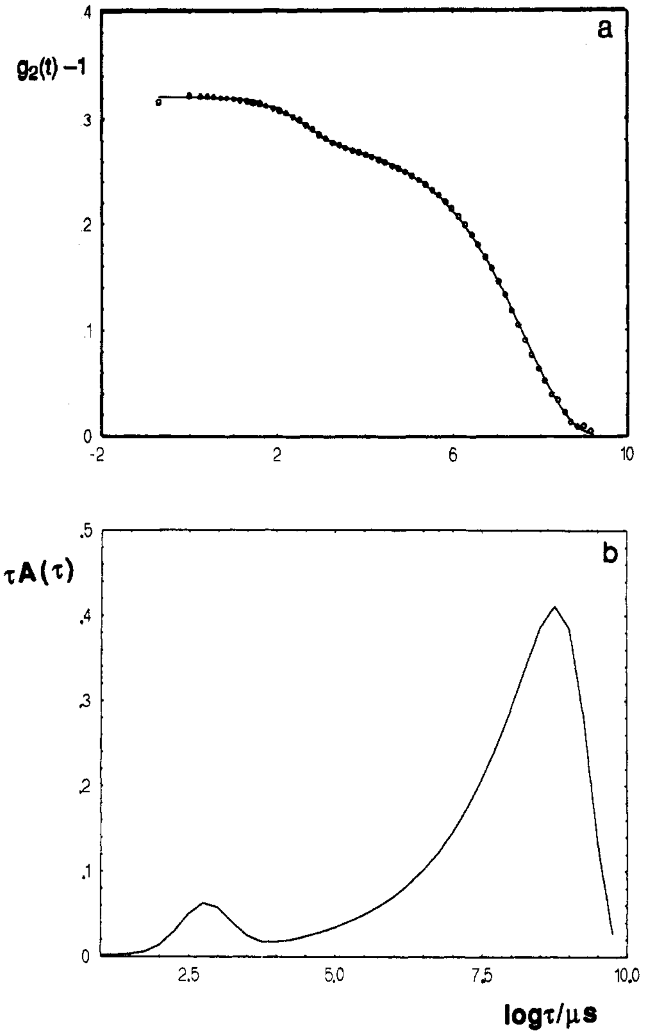

**Figure 15.** (a) Polarized intensity autocorrelation function for polystyrene in toluene; $C = 0.9$ g/mL at 30 °C and $\theta = 90°$. A narrow $q^2$-dependent mode precedes the broad $q$-independent mode. (b) Corresponding relaxation time distribution obtained from a Gauss-GEX analysis (see text).

These observations may be explained if we assume a two-step diffusion of the solvent through the transient network. In a first step, the solvent diffuses through the free volume in the frozen network. Only a small part of the concentration fluctuations can relax in this way due to the limited availability of free volume. The amplitude of this decay is expected to depend on the size of the solvent molecule, which could explain the lack of such a relaxation in the case of the much larger DOP molecule. In a second step, the solvent locally swells and deswells the transient network. The rate of this second step is determined either by the relaxation of the polymer backbone or by the diffusion rate of the solvent, whichever is slowest. A theoretical account of such a two-step relaxation sequence is given by Jäckle et al.[20,21] in terms of a frequency-dependent chemical potential. A semiquantitative comparison of the results on the polystyrene/toluene system with this theory is given elsewhere.[22] In fact, a third step may be involved in the relaxation of the concentration fluctuations, i.e., the structural relaxation of the transient network. This process dominates the correlation functions measured on semidilute solutions of high molar mass polymers in thermodynamically poor solvents.[14] However, in the case of concentrated solutions its effect will be small.

If the $q^2$-dependent relaxation is due to cooperative diffusion, the relaxation time is related to the inverse osmotic compressibility and the friction coefficient, $f$, per gram polymer in the following way:[23,24]

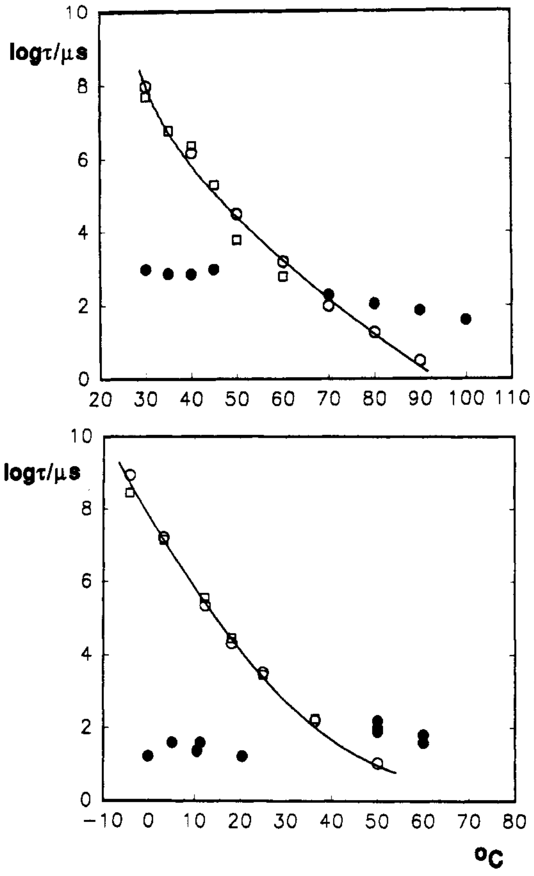

**Figure 16.** Characteristic relaxation times from polarized ($V_V$) and depolarized ($V_H$) measurements plotted as a function of temperature for PS in toluene $C = 0.9$ g/mL (a) and $C = 0.8$ g/mL (b). The open circles and squares represent the $q$-independent mode ($\tau_{or}$) obtained from depolarized and polarized measurements, respectively, while the filled circles represent the $q^2$-dependent data ($\tau_{con}$) obtained from polarized measurements. (The solid lines are guides to the eye.)

$$\tau q^2 \sim [(1-\phi)^2(\delta\pi/\delta c)/f]^{-1} \tag{4}$$

where $\phi$ is the volume fraction of the polymers. The osmotic compressibility can be estimated from the scattered light intensity due to the concentration fluctuations. In the concentration and temperature range studied here, $(\delta\pi/\delta c)$ is observed to be independent of the temperature so that the temperature dependence of $\tau$ enters through the temperature dependence of $f$. With toluene as solvent the temperature dependence of $f$ is rather weak, when $\tau_{con}$ is both slower and faster than the density fluctuations. In the case of DOP it is much stronger. For the three PS/DOP concentrations studied the value of $[(1-\phi)^2(\delta\pi/\delta c)]$ is similar in magnitude, implying that the variation in $\tau$ with concentration is mainly due to the variation in $f$.

A detailed investigation of the cooperative diffusion coefficient of polystyrene in DOP over a wide concentration and temperature range will be reported elsewhere. This study shows that the similar concentration shifts for the relaxation rates of concentration and density fluctuations in the higher concentration range can be explained in the framework of free volume theory.

**Acknowledgment.** This work has been supported by the Swedish Natural Science Research Council (NFR). T.N. wishes to thank the CNRS for a travel grant in connection with his stay in Uppsala. Thanks are due to Dr. L. Dvoranek for performing the thermal polymerization of polystyrene in DOP.

## References and Notes

(1) Fytas, G.; Floudas, G.; Ngai, K. L. *Macromolecules* **1990**, *23*, 1104.

(2) Floudas, G.; Fytas, G.; Fischer, E. W. *Macromolecules* **1991**, *24*, 1955.

(3) Brown, W.; Johnsen, R. M.; Konak, C.; Dvoranek, L. *J. Chem. Phys.* **1991**, *95*, 8568.

(4) Floudas, G.; Fytas, G.; Brown, W. *J. Chem. Phys.* **1992**, *96*, 2164.

(5) Koch, T.; Strobl, G.; Stuhn, B. *Macromolecules* **1992**, *25*, 6255.

(6) Brown, W.; Mortensen, K.; Floudas, G. *Macromolecules* **1992**, *25*, 6904.

(7) Wang, C. H.; Fischer, E. W. *J. Chem. Phys.* **1985**, *82*, 632.

(8) Gapinski, J.; Fytas, G.; Floudas, G. *J. Chem. Phys.* **1992**, *96*, 6311.

(9) *Dynamic Light Scattering*; Brown, W., Ed.; Oxford University Press: Oxford, U.K., 1993.

(10) Floudas, G.; Steffen, W.; Giebel, L.; Fytas, G. *Progr. Colloid Polym. Sci.* **1993**, *91*, 124.

(11) Floudas, G.; Higgins, J. S.; Fytas, G. *J. Chem. Phys.* **1992**, *96*, 7672.

(12) Patterson, G. D. *Adv. Polym. Sci.* **1983**, *48*, 125.

(13) Floudas, G.; Steffen, W.; Brown, W.; Fischer, E. W. *J. Chem. Phys.* **1993**, *99*, 695.

(14) Nicolai, T.; Brown, W.; Hvidt, S.; Heller, K. *Macromolecules* **1990**, *23*, 5088.

(15) Jakes, J. *Czech. J. Phys. B* **1988**, *38*, 1305.

(16) Provencher, S. W. *Makromol. Chem.* **1979**, *180*, 201.

(17) Peters, R. In *Dynamic Light Scattering*; Brown, W., Ed.; Oxford University Press: Oxford, U.K., 1993.

(18) Yamakawa, H. *Modern Theory of Polymer Solutions*; Harper & Row: New York, 1971.

(19) Lindsey, C. P.; Patterson, G. D.; Stevens, J. R. *J. Polym. Sci.* **1979**, *17*, 1547.

(20) Jäckle, J.; Frisch, H. L. *J. Polym. Sci.* **1985**, *23*, 675.

(21) Jäckle, J.; Pieroth, M. *J. Phys.: Condens. Matter* **1990**, *2*, 4963.

(22) Konak, C.; Brown, W. *J. Chem. Phys.* **1993**, *98*, 9014.

(23) Vink, H. J. *J. Chem. Soc. Faraday Trans.* **1985**, *81*, 1725.

(24) Geissler, E. In *Dynamic Light Scattering*; Brown, W., Ed.; Oxford University Press: Oxford, U.K., 1993.